High average brightness water window source for short-exposure cryomicroscopy

D. H. Martz,[1] M. Selin,[1] O. von Hofsten,[1] E. Fogelqvist,[1] A. Holmberg,[1] U. Vogt,[1] H. Legall,[2] G. Blobel,[2] C. Seim,[3] H. Stiel,[2] and H. M. Hertz[1,*]

[1]*Biomedical and X-Ray Physics, Department of Applied Physics, KTH Royal Institute of Technology/Albanova, Stockholm 10691, Sweden*

[2]*Max-Born-Institute, Max-Born-Straße 2A, Berlin 12489, Germany*

[3]*Institute of Optics and Atomic Physics—Analytical X-ray physics, Technical University-Berlin, Berlin 10623, Germany*

**Corresponding author: hertz@biox.kth.se*

Received July 13, 2012; revised September 18, 2012; accepted September 19, 2012; posted September 20, 2012 (Doc. ID 171680); published October 22, 2012

Laboratory water window cryomicroscopy has recently demonstrated similar image quality as synchrotron-based microscopy but still with much longer exposure times, prohibiting the spread to a wider scientific community. Here we demonstrate high-resolution laboratory water window imaging of cryofrozen cells with 10 s range exposure times. The major improvement is the operation of a $\lambda = 2.48$ nm, 2 kHz liquid nitrogen jet laser plasma source with high spatial and temporal stability at high average brightness $>1.5 \times 10^{12}$ ph/(s × sr × μm^2 × line), i.e., close to that of early synchrotrons. Thus, this source enables not only biological x-ray microscopy in the home laboratory but potentially other applications previously only accessible at synchrotron facilities.

OCIS codes: 340.7460, 340.7480.

Microscopy in the water window ($\lambda = 2.3$–4.4 nm; $E = 284$–540 eV) allows for imaging of unstained intact cells in their near-native environment with unprecedented resolution and contrast [1]. Within the last few years, synchrotron-based microscopy has demonstrated significant progress delivering results of high biological relevance with second-range exposure times [2,3]. Laboratory microscopy now produces images with synchrotron quality but with longer exposure times [4–6]. We note that already the modest average spectral brightness of early 2nd generation bending magnet synchrotron radiation sources of 10^{12}–10^{13} ph/(s × mm^2 × mrad^2 × 0.1% BW) was enough to enable water window x-ray microscopy with exposure times of a few to a few tens of seconds [7], sufficiently short to make the technique attractive. Unfortunately, no tabletop source has emerged with sufficient average brightness and stability to demonstrate laboratory water window microscopy with such short exposure times.

To date, only two types of laboratory sources, gas discharges and laser plasmas, have been used for water window microscopy in the laboratory, both with long exposure times. A nitrogen pinch discharge operating at the $\lambda = 2.88$ nm helium-like line has demonstrated an average line brightness of 4×10^9 ph/(s × mm^2 × mrad^2 × line) [8], while the laser plasmas have demonstrated 4×10^{10} ph/(s × mm^2 × mrad^2 × line) at the $\lambda = 2.48$ nm hydrogen-like nitrogen line using liquid jet targets [9]. Given the 0.1–0.2% BW ($\lambda/\Delta\lambda \approx 500$–$1000$) of the lines [10], the laboratory source spectral brightnesses are still significantly below that of the early bending magnet sources. Consequently, with these sources, exposure times have been in the few minute range for biological microscopy [4,5] and in few to ten second range for dry objects [8].

In this Letter, we demonstrate laboratory water-window x-ray microscopy of a cryofrozen biological specimen with 10 s range exposure times, i.e., approaching that of early bending magnet based microscopes. Figure 1 shows the experimental arrangement, the Stockholm laboratory x-ray microscope [11,4]. It consists of the laser plasma source, a $\lambda/\Delta\lambda \approx 300$ Cr/V normal-incidence multilayer condenser mirror, a cryogenic sample holder, an $N = 500$ zone and $dr_n = 30$ nm outer zone width zone plate, and a CCD detector, all in vacuum. The short exposure times were enabled by the operation of a 2 kHz/200 W slab laser driven liquid jet laser plasma source with high long-term stability and high average brightness. In a parallel development a lower source power sister microscope is under construction in Berlin, presently still limited to 1–2 min exposure times on dry objects [12].

The laser plasma source utilizes a liquid nitrogen jet as a regenerative target and exploits the $\lambda/\Delta\lambda > 500$ hydrogen-like (NVII, $1s$-$2p$) line emission at $\lambda = 2.478$ nm [9]. Stable $d = 20$ μm diameter jets are formed by a fused-silica capillary nozzle, driven by a 10–20 atm pressure resulting in a $v = 60$ m/s jet speed and an angular stability of <1 mrad. This is sufficient to supply fresh target material with appropriate spatial stability for 2 kHz operation. The plasma is formed by focusing the $\lambda = 1064$ nm beam from the 2 kHz, 100 mJ, 600 ps Nd:YAG laser onto the jet. This 200 W laser is a compact master oscillator power-amplifier (MOPA) all diode pumped system comprised of a diode seeder, a regenerative amplifier, and three successive slab amplifiers [13]. After cylindrical compensation of the asymmetric beam, we typically focus to a 6.5×13 μm^2 full width at half-maximum (FWHM) spot with >65% of the focal plane energy in a 12×21 μm^2 area. The resulting peak intensity at the target is estimated to be 0.5–1×10^{14} W/cm^2. From a simple equilibrium and equivalent black-body temperature argument [14] and assuming 50% absorption, this would result in an approximatly 150 eV plasma with a corresponding peak emission at 400–450 eV, close to the optimum for the 500 eV NVII line.

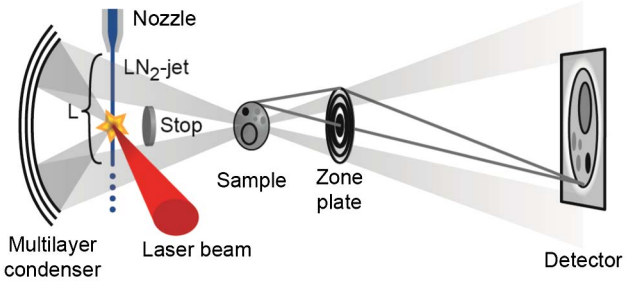

Fig. 1. (Color online) Stockholm soft x-ray microscope with the high-power liquid jet source, a Cr/V multilayer condenser mirror, nickel zone plate optics, and CCD detector.

Avoiding spatial and temporal instabilities is essential for producing the high average brightness necessary for short-exposure microscopy. At our power levels, the laser must be focused as far away from the nozzle tip as possible to avoid fluid mechanical instabilities of the jet due to thermal loading from the hot plasma. Still, it must be focused on the continuous region of the jet before it breaks up into droplets to obtain high temporal stability. The break up length for the natural drop formation of a liquid jet is given by $L \approx C\nu[(\sqrt{\rho d^3/\sigma}) + (3\eta d/\sigma)]$ [15] and varies between 3.5 mm ($T = 63$ K, LN2 freezing point at NTP) and 3.9 mm ($T = 77$ K, boiling point at NTP) for our liquid nitrogen jet parameters. The density ρ, viscosity η, and surface tension σ are functions of temperature given by [16], and we assume $C = 3.5$ according to our experimental experience for these types of nozzles [15]. We typically operate close to the droplet formation point at $L = 3$ mm, as monitored by a visible-light microscope and, counterintuitively, close to the freezing point at $T \approx 64$–65 K. The reason is the strong temperature dependence of the viscosity, which lowers the Reynold's number $\mathrm{Re} = \nu\eta d$ by nearly a factor of 2 in the 77 – 64 K range. Although Re cannot be used to predict turbulence accurately due to a short nozzle length, Re is a good indicator of the liquid jet's probability to become unstable and, thus, its susceptibility to disturbances. Since we operate at a high Re (2500), minor disturbances may also result in nonstable (spraying) jets. To provide a stable high-density target, the jet is therefore maintained just above the freezing point. With these parameters, we obtain a sufficiently stable laser plasma to allow long-term high brightness operation and short exposure times.

Figure 2 summarizes the spectral and spatial characterization of the source. The spectrum was quantitatively measured with a calibrated 10,000 line/mm slit-grating spectrograph [17]. Figure 2(a) shows a typical spectrum taken at 100 mJ pulse energy. The peak value of the NVII ($1s$-$2p$) $\lambda = 2.48$ nm line is 1.1×10^{10} ph/(pulse×sr×pm). The spectral resolution is limited by the spectrograph arrangement to $\lambda/\Delta\lambda \approx 100$, greatly exceeding the actual emission line width. The asymmetry in the line profile is probably due to a slight source asymmetry in combination with a small contribution of the NVI ($1s^2$-$1s3p$) emission line at 2.490 nm [10]. To determine the photon flux of the 2.48 nm line we integrate over 2 × FWHM of the line, resulting in 5.5×10^{11} ph/(pulse × sr × line). The resulting ratio between the NVII line and helium-like NVI ($1s^2$-$1s2p$) line is in agreement with the expected plasma temperature. Figure 2(b) shows the average photon flux for the $\lambda = 2.48$ nm line versus laser power (74 data points). The flux scales linearly with laser power in this range and when the source is operated at 2 kHz (200 W) a maximum of 1.1×10^{15} ph/(s × sr × line) is measured.

To determine the average spectral brightness of the source, the source size was measured using the normal-incidence multilayer mirror. The $\lambda/\Delta\lambda \approx 300$ mirror bandpass allows for selective imaging of the $\lambda = 2.48$ nm line. Synchrotron measurements verified the proper spectral match between the mirror reflectivity maximum (0.6%) and the emission line. The source size is typically 14 × 20 μm^2 FWHM. In Fig. 2(c), the photon flux and size data are combined, resulting in quantitative source brightness with a maximum average line brightness $>1.5 \times 10^{12}$ ph/(s × sr × μm^2 × line). For comparison we note that this corresponds to a spectral brightness of >0.7–1.5× 10^{12} ph/(s × mm^2 × mrad^2 × 0.1% BW), similar to early bending magnet synchrotrons.

For applications like microscopy, the stability of the source is of equal importance as the brightness. Any temporal or spatial instability reduces the effective average brightness and thus increases exposure times. Furthermore, instabilities make alignment difficult and decrease image quality due to increased background. For the present laser-plasma source, we measure the spatial stability to $< \pm 5$ μm and the exposure-to-exposure intensity fluctuation to $< \pm 5\%$ (10 s averages). All brightness data given above are determined from repeated measurements to provide average numbers useful for microscopy.

The Stockholm soft x-ray microscope was operated with the source, as shown in Fig. 1. The $\lambda = 2.48$ nm wavelength provides high water window transmission

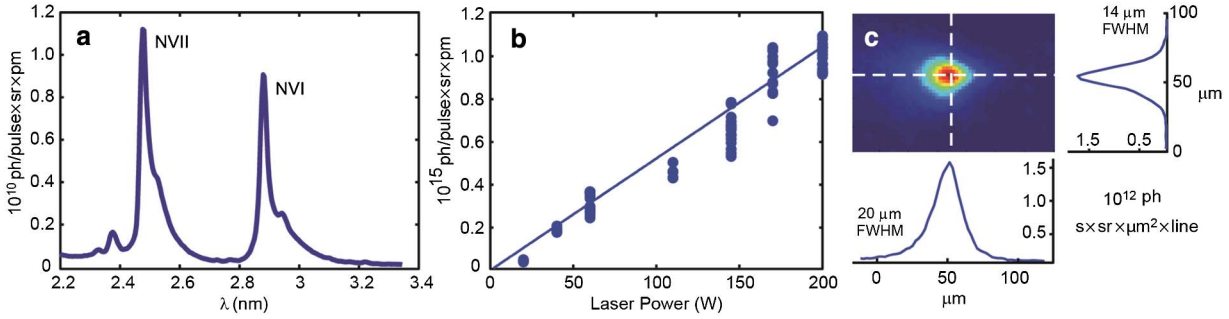

Fig. 2. (Color online) (a) Quantitative per-pulse liquid nitrogen jet spectrum with the hydrogen-like (NVII) and helium-like (NVI) peaks at $\lambda = 2.478$ nm (500 eV) and $\lambda = 2.879$ nm (431 eV). (b) The $\lambda = 2.48$ nm line emission photon flux as a function of laser power. (c) Imaging of the 2.48 nm emitting region with cuts showing the quantitative soft x-ray line brightness.

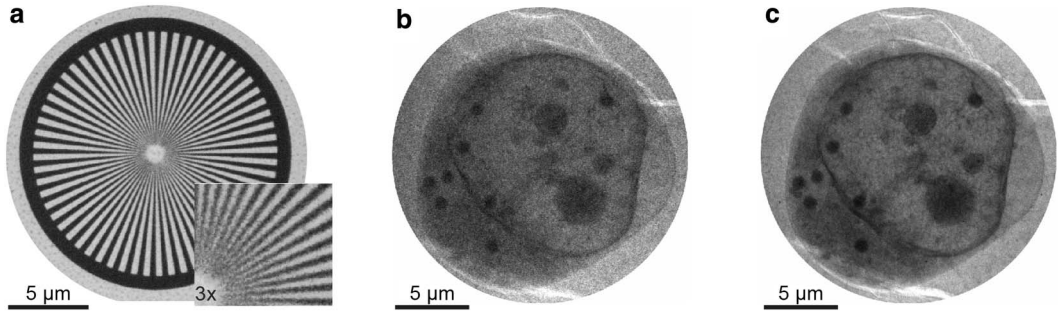

Fig. 3. (a) Water window microscopy of a gold Siemens star at 10 s exposure time. (b) Cryofixed human B-cell at 10 s exposure time. (c) Cryo-fixed human B-cell at 60 s exposure time.

and the $\lambda/\Delta\lambda > 500$ bandwidth is well within the condenser bandwidth and is sufficient for $N = 500$ zone plate imaging without chromatic aberration. The resolution was tested by imaging a 17 μm diameter gold Siemens star with a center line width of 25 nm (50 nm full period). Figure 3(a) shows the result, taken at a magnification of 667 with a 10 s exposure time at half source power. With this magnification, each CCD pixel corresponds to ~20 nm, i.e., approximately the Nyquist limit for the 30 nm zone plate. Lines and spaces can be observed down to 50 nm, limited by noise, while for 30 s exposures, 40 nm L/S are observed. Figures 3(b) and 3(c)demonstrate bioimaging. Here a cryofrozen human B-cell is recorded with a magnification of 1000 at 10 and 60 s, respectively, showing nuclear membrane, nucleoli, and what is believed to be protein-dense granules. The images have been smoothed so that the effective pixel size is 20 nm, corresponding to the resolution of the zone plate. Without sample, a 10 s exposure typically results in 250–300 photons per 20 nm pixel at the detector. With the samples in Figs. 3(b) and 3(c), the photon numbers are 35 and 150, respectively, indicating that a somewhat thick water layer remained after the sample preparation.

In summary, we have demonstrated a narrow band, tabletop water window source with sufficient average brightness and stability to allow x-ray microscopy with 10 s range exposure times. Such short exposure times are especially important for biological x-ray microscopy, where screening of large sample volumes or tomography are practically impossible with systems having long alignment and/or exposure times. Thus, this source has potential to enable the spread of x-ray microscopy as well as other brightness-dependent x-ray methods to the small to medium scale laboratory.

We thank D. Esser and M. Höfer for their efforts on the laser and M. Bertilson for valuable discussions. This work was supported by the Wallenberg Foundation, the Swedish Research Council, and the Swedish Foundation for Strategic Research.

References

1. A. Sakdinawat and D. Attwood, Nat. Photonics **4**, 840 (2010).
2. M. Uchida, G. McDermott, M. Wetzler, M. A. Le Gros, M. Myllys, C. Knoechel, A. E. Barron, and C. A. Larabell, Proc. Natl. Acad. Sci. USA **106**, 19375 (2009).
3. G. Schneider, P. Guttmann, S. Heim, S. Rehbein, F. Mueller, K. Nagashima, J. B. Heymann, W. G. Müller, and J. G. McNally, Nat. Methods **7**, 985 (2010).
4. M. Bertilson, O. von Hofsten, U. Vogt, A. Holmberg, A. E. Christakou, and H. M. Hertz, Opt. Lett. **36**, 2728 (2011).
5. H. M. Hertz, O. von Hofsten, M. Bertilson, U. Vogt, A. Holmberg, J. Reinspach, D. Martz, M. Selin, A. E. Christakou, J. Jerlström-Hultqvist, and S. Svärd, J. Struct. Biol. **177**, 267 (2012).
6. D. B. Carlson, J. Gelb, V. Palshin, and J. E. Evans, "Laboratory-based cryogenic soft x-ray tomography," Microsc. Microanal. (to be published).
7. G. Schmahl, D. Rudolph, B. Niemann, P. Guttmann, J. Thieme, G. Schneider, C. David, M. Diehl, and T. Wilhein, Optik **93**, 95 (1993).
8. M. Benk, K. Bergmann, D. Schäfer, and T. Wilhein, Opt. Lett. **33**, 2359 (2008).
9. P. A. C. Jansson, U. Vogt, and H. M. Hertz, Rev. Sci. Instrum. **76**, 43503 (2005).
10. T. Wilhein, D. Hambach, B. Niemann, M. Berglund, L. Rymell, and H. M. Hertz, Appl. Phys. Lett. **71**, 190 (1997).
11. P. Takman, H. Stollberg, G. A. Johansson, A. Holmberg, M. Lindblom, and H. M. Hertz, J. Microsc. **226**, 175 (2007).
12. H. Legall, G. Blobel, H. Stiel, W. Sandner, C. Seim, P. Takman, D. H. Martz, M. Selin, U. Vogt, H. M. Hertz, D. Esser, H. Sipma, J. Luttmann, M. Hofer, H. D. Hoffmann, S. Yulin, T. Feigl, S. Rehbein, P. Guttmann, G. Schneider, U. Wiesemann, M. Wirtz, and W. Diete, Opt. Express **20**, 18362 (2012).
13. Institute for Laser Technology, www.ilt.fhg.de.
14. D. Attwood, *Soft X-rays and Extreme Ultraviolet Radiation* (Cambridge, 2000), Chap. 6.
15. B. A. M. Hansson, M. Berglund, O. Hemberg, and H. M. Hertz, J. Appl. Phys. **95**, 4432 (2004).
16. http://webbook.nist.gov/chemistry.
17. T. Wilhein, S. Rehbein, D. Hambach, M. Berglund, L. Rymell, and H. M. Hertz, Rev. Sci. Instrum. **70**, 1694 (1999).